# Modeling percolation in high-aspect-ratio fiber systems. I. Soft-core versus hard-core models

L. Berhan[1,*] and A. M. Sastry[2]
[1]*Department of Mechanical, Industrial and Manufacturing Engineering, University of Toledo, Toledo, Ohio 43606-3390, USA*
[2]*Department of Mechanical, Biomedical and Materials Science and Engineering, University of Michigan, Ann Arbor, Michigan 48109-2125, USA*
(Received 28 August 2006; published 30 April 2007)

Numerical and analytical studies of the onset of percolation in high-aspect-ratio fiber fiber systems such as nanotube reinforced polymers available in the literature have consistently modeled fibers as penetrable, straight, capped cylinders, also referred to as spherocylinders. In reality, however, fibers of very high-aspect ratio embedded in a polymer do not come into direct physical contact with each other, let alone exhibit any degree of penetrability. Further, embedded fibers of very high-aspect ratio are often actually wavy, rather than straight. In this two-part paper we address these critical differences between known physical systems, and the presently used spherocylinder percolation model. In Paper I we evaluate the effect of allowing penetration of the model fibers on simulation results by comparing the soft-core and the hard-core approaches to modeling percolation onset. We use Monte Carlo simulations to investigate the relationship between percolation threshold and excluded volume for both modeling approaches. Our results show that the generally accepted inverse proportionality between percolation threshold and excluded volume holds for both models. We further demonstrate that the error introduced by allowing the fibers to intersect is non-negligible, and is a function of both aspect ratio and tunneling distance. Thus while the results of both the soft-core model and hard-core assumptions can be matched to select experimental results, the hard-core model is more appropriate for modeling percolation in nanotubes-reinforced composites. The hard-core model can also potentially be used as a tool in calculating the tunneling distance in composite materials, given the fiber morphology and experimentally derived electrical percolation threshold. In Paper II we investigate the effect of the waviness of the fibers on the onset of percolation in fiber reinforced composites.

DOI: 10.1103/PhysRevE.75.041120 PACS number(s): 64.60.−i, 72.80.Tm

## I. INTRODUCTION

Percolation in carbon nanotube-reinforced composites is of high interest because of the potential to create electrically and/or thermally conductive systems with an extremely low mass of particles. Indeed, experimental findings in nanotube-reinforced polymeric [1–11] and ceramic [12] matrix materials have shown that conductivity follows a percolationlike behavior. Specifically, at a relatively low concentration of nanotubes, the conductivity dramatically increases; near the percolation threshold, the conductivity follows the classic scaling law of percolation theory (Table I).

Analytical and numerical tools presently available to model percolation onset stem from a variety of disciplines, and span both two-dimensional (2D) and 3D systems of fibers and fiberlike objects. The earliest models were developed to study cellulose [13,14] and other biological fibers. More recent work, by Sastry and co-workers, has resulted from the study of energy storage materials [15–22], and has also included studies on mechanical properties of fibrous arrangements [23–25].

Table II summarizes key literature on geometric percolation studies in random three-dimensional fibrous materials [26–31], and includes work in systems of ellipses, since fibers can often be conveniently modeled as high-aspect-ratio (i.e., high values of length by radius) ellipses in numerical implementations in which singularities must be reduced [15]. In these treatments, percolation is defined as the formation of a connected cluster that spans a representative volume element. Geometric percolation and electrical percolation are often treated as coincident in the literature, since the percolationlike conductivity behavior is generally attributed to the formation of a physically connected path of the conducting particles within the matrix. While this phenomenon is true of some materials in which conducting particles coalesce and produce a continuous conducting network, nanotubes embedded in a polymer matrix are not in physical contact. The primary charge transport mechanism in nanotubes reinforced composites is electron tunneling [32,33].

In composites in which the primary charge transfer mechanism is tunneling, all objects are electrically connected. Further, the objects are not connected physically, and therefore there is no geometric percolation threshold. These two factors are incompatible with classic percolation theory. This inconsistency is often ignored in discussions of the conductivity of composite materials, and a classic geometric model of penetrable particles is widely used to model the onset of their electrical percolation. Balberg and co-workers [34–36] recently studied percolation and tunneling in composite materials. Using capacitance probe microscopy they found that the percolating cluster consisted of nearest neighbor particles and thus the electrical conductivity of carbon black copolymer composites was well described by geometric percolation. They concluded that metal-insulator composite materials behave like "bona fide percolating systems" when only nearest neighbor tunneling contributes to the conduction. In composite materials in which the conducting particles do not coalesce, the percolationlike behavior can thus

*Author to whom correspondence should be addressed.

 

TABLE I. Experimentally derived percolation thresholds for composites reinforced with single walled nanotubes (SWNT) and multiwalled nanotubes (MWNT) from selected literature.

| Authors | Year | Ref. | Carbon nanotube type | Matrix type | Nanotube density ($g/cm^3$) | Percolation threshold | | Dispersion |
|---|---|---|---|---|---|---|---|---|
| | | | | | | wt % | vol % | |
| Coleman *et al.* | 1998 | [5] | | PMPV | | 8.4 | | |
| Sandler *et al.* | 1999 | [10] | | epoxy | | 0.025–0.04 | | nonuniform |
| Yoshino *et al.* | 1999 | [11] | MWNT | PAT6 | | | 5.9 | |
| Benoit *et al.* | 2001 | [2] | SWNT | PMMA | 1.3 | 0.33 | 0.33 | |
| Andrews *et al.* | 2002 | [1] | MWNT | poly(propylene) | | | 0.05 | uniform |
| Kilbride *et al.* | 2002 | [6] | MWNT | PmPV, PVA | | 0.055 | | |
| Biercuk *et al.* | 2002 | [3] | SWNT | epoxy | | 0.1–0.2 | | uniform |
| Kymakis, Alexandou, and Amaratunga | 2002 | [7] | SWNT | P3OT | | 11 | | |
| Potschke, Fornes, and Paul | 2002 | [9] | MWNT | polycarbonate | | 1.0–2.0 | | |
| Blanchet, Fincher, and Gao | 2003 | [4] | SWNT | polyaniline | | 0.3 | | uniform |
| Ounaies *et al.* | 2003 | [8] | SWNT | polyimide | 1.33–1.4 | 0.05 | 0.05 | uniform |

be attributed to the formation of an effective percolating cluster in which nearest neighbor particles are within a certain tunneling range from one another. The electrical percolation onset depends not only on particle geometry and distribution, but also on parameters that affect tunneling distance.

A more suitable approach to modeling percolation in these systems is the hard-core model in which each conducting inclusion is modeled as an impenetrable hard core surrounded by a soft shell, where the hard core represents the actual inclusion and the thickness of the surrounding penetrable soft shell is related to the tunneling distance. The hard-core approach is widely used to model microemulsions [37,38], and liquids in which spherical particles are considered. However, treatments using the hard-core approach to model percolation of fibrous systems are limited to the study of low-aspect-ratio objects.

Balberg and Binenbaum [39] used Monte Carlo simulations to investigate the average critical number of bonds per site, $B_c$, for three-dimensional continuum systems of spheres and cylinders in the hard-core—soft-core transition. Their results led to the conjecture that $B_c$ was dimensionally invariant for long cylinders, however, due to computation constraints the ratio of length to radius (i.e., aspect ratio) in their simulations was limited to 10. Ogale and Wang [40] used a hard-core model to study percolation in short fiber reinforced composites and found that experimentally obtained values of the percolation threshold were in good agreement with the results of Monte Carlo simulations. Their results support the conjecture that a composite behaves as a genuine percolating system when only interactions between nearest neighbor fibers are considered. However, their simulations were limited to systems where the aspect ratios of the hard core were between 12 and 50. Their results are therefore not directly applicable to composites reinforced with very high-aspect-ratio fibers, such as nanotube reinforced composites.

A hard-core numerical modeling approach for high-aspect-ratio fibers is very computationally intensive. A popular approach to modeling the percolation behavior of composites with high-aspect-ratio fibers is to consider the geometric percolation of soft-core (i.e., fully permeable) rods and to assume that the onset of both geometric and electrical percolation occur simultaneously. Several researchers have studied the percolation in nanotubes reinforced composites by modeling each nanotube as a rigid, straight, penetrable spherocylinder (i.e., a cylinder with hemispheric end caps) (e.g., [8,41,42]), most without noting the inconsistencies between the physical system and the soft-core approach. Despite the differences between a soft-core spherocylinder network model and the actual nanotube reinforced composite, the soft-core model has been shown to predict percolation thresholds that are in very good agreement with experimental results. This apparent validation of the soft-core model may serve as an explanation of why the applicability of the soft-core spherocylinder model to the specific problem of nanotube reinforced composite has not been addressed in the literature.

In this paper, we investigate the applicability of the soft-core vs the hard-core approach to modeling percolation in high-aspect-ratio fibrous systems and composites. We propose an analytical approach to studying systems of very high aspect ratios (on the order of hundreds or thousands) based on the results of simulations performed at lower-aspect-ratios. The specific objectives of this work are (i) to use Monte Carlo simulations to find the percolation threshold of systems of randomly oriented straight cylinders using both hard-core and soft-core approaches, (ii) to develop an analytical approach for the determination of onset of percolation

TABLE II. Key percolation studies in three-dimensional random fibrous materials.

| Authors | Year | Ref. | Arrangement | Objects | Contribution | Approach |
|---|---|---|---|---|---|---|
| Balberg, Binenbaum, and Wagner | 1984 | [27] | isotropic | capped cylinders | First study of percolation of random objects in three dimensions. | Monte Carlo simulations |
| Balberg *et al.* | 1984 | [26] | isotropic | capped cylinders | Presented the conjecture that percolation threshold for a system of identical objects in three dimensions is inversely proportional to excluded volume of one object. | Monte Carlo simulations |
| Bug, Safran, and Webman | 1985 | [28] | isotropic | capped cylinders | Confirmed excluded volume rule and showed constant of proportionality equals one in slender rod limit. | cluster expansion |
| Neda, Florian, and Brechet | 1999 | [29] | isotropic | capped cylinders | Performed Monte Carlo simulations of 3D stick systems using correct isotropic distribution and confirmed excluded volume theory. | Monte Carlo simulations |
| Yi and Sastry | 2004 | [30] | isotropic | ellipsoids | Presented analytical approximation for the percolation threshold of two- and three-dimensional arrays of overlapping ellipsoids. | series expansion |
| Yi, Wang, and Sastry | 2004 | [31] | Uniform distribution in $x-y$ plane. Range of distributions fromparallel to random in $z$ direction. | ellipsoids | Provided comparisons of cluster sizes, densities, and percolation points for two- and three-dimensional systems of overlapping ellipsoids to investigate the range of applicability of a 2D model for predicting percolation in thin three-dimensional systems. | Monte Carlo simulations |

in ct ratio fiber systems, and (iii) to compare the results of both soft-core and hard-core approaches to experimental data for nanotubes reinforced composites.

In Sec. II we present descriptions of the classic soft-core spherocylinder model and the hard-core approach. In Sec. III we use Monte Carlo simulations to find the percolation threshold for three-dimensional systems for randomly oriented straight spherocylinders using both modeling approaches and present relationships between percolation threshold and excluded volume. In Sec. IV we compare the results of both the soft-core and hard-core models to experimental results for nanotubes reinforced composites reported in the literature. These results are discussed in the context of the applicability of the models to nanotube-reinforced composites in Sec. V.

## II. MODELING APPROACH

### A. Soft-core spherocylinder model

Monte Carlo simulations can be used to numerically determine percolation onset in 3D fiber systems, using either a soft-core or hard-core approach. However, calculations become prohibitively intensive for arrays of fibers of very high aspect ratio. Thus we first return to a semiempirical, analytical result by Balberg *et al.* [26] as a starting point in our investigation. This model considers the percolation of soft-core (interpenetrable) rigid spherocylinders, randomly oriented in three dimensions. These "sticks" are assumed to be straight cylinders of length $L$ and radius $R$, with hemispheric end caps of radius $R$ to allow comparison of results in the $L/R \to 0$ limit with well-established results for spheres. The derivation begins with the assumption that the number of objects per unit volume at percolation $q_p$ is inversely proportional to the excluded volume $V_{\mathrm{ex}}$ of one of the objects, i.e.,

$$q_p \propto \frac{1}{V_{ex}}. \tag{1}$$

The excluded volume is the volume around the object into which the center point of an identical object is prohibited, if the two are not to overlap. In general, for spherocylinders of length $L$ and radius $R$, the excluded volume is given by

$$V_{ex} = \frac{32\pi}{3}R^3\left[1 + \frac{3}{4}\left(\frac{L}{R}\right) + \frac{3}{8\pi}\langle \sin(\theta)\rangle\left(\frac{L}{R}\right)^2\right], \tag{2}$$

where $\langle \sin(\theta)\rangle$ is the average value of $\sin(\theta)$ for two sticks and $\theta$ is the angle between them. For a random distribution $\langle \sin(\theta)\rangle = \frac{\pi}{4}$, thus

$$V_{ex} = \frac{32\pi}{3}R^3\left[1 + \frac{3}{4}\left(\frac{L}{R}\right) + \frac{3}{32}\left(\frac{L}{R}\right)^2\right]. \tag{3}$$

The volume of a single spherocylinder can be written as

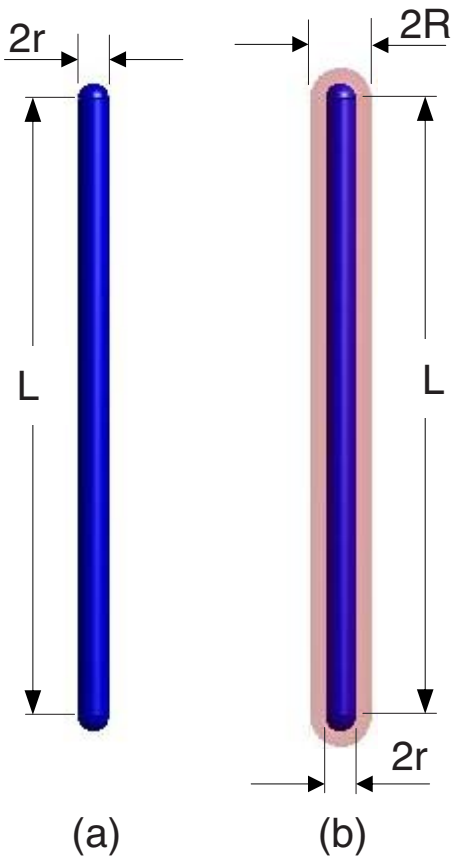


FIG. 1. (Color online) (a) Soft-core model and (b) hard-core model with soft shell of radius $R$ for a spherocylinder of length $L$ and radius $r$.

$$V = \frac{4\pi}{3}R^3 + \pi R^2 L. \tag{4}$$

In this paper we define aspect ratio as the ratio of length to radius, i.e., $L/R$. It has been shown previously [28] using a cluster expansion method, and supported by numerical simulations [29], that in the slender rod limit (as $R/L \to 0$) the constant of proportionality in Eq. (1) is unity, therefore for very high-aspect-ratio fibers the analytical solution for $q_p$ is often expressed as

$$q_p = \frac{1}{V_{ex}}. \tag{5}$$

Since $q_p$ is the number of objects per unit volume at percolation, the analytical solution for the volume fraction of high-aspect-ratio fibers at the percolation threshold is often written as

$$\phi_c = \frac{V}{V_{ex}}. \tag{6}$$

### B. Hard-core spherocylinder model

Figure 1 shows the soft-core and hard-core spherocylinder models. The soft-shell model [Fig. 1(a)] has length $L$ and radius $r$ and is assumed to be fully penetrable, so that objects are allowed to overlap and penetrate each other. The hard-core model [Fig. 1(b)] has an impenetrable core of radius $r$ and length $L$ with hemispheric end caps of radius $r$ along with a surrounding spherocylindrical soft shell of length $L$ and radius $R$ and hemispheric end caps of radius $R$. The hard cores are not permitted to overlap, and two hard-core objects are considered to intersect if the penetrable soft shells overlap.

We define the parameter $t$ as the ratio of the radius of the core to the outer radius of the soft shell,

$$t = \frac{r}{R}. \tag{7}$$

We can express the soft-core limit as $t=0$ and the hard-core limit is given by $t=1$.

Since the interior spherocylinder is impenetrable, the excluded volume of the hard-core object is equal to the excluded volume of the soft shell minus that of the hard core. The excluded volume can be written as

$$V_{ex} = \frac{32\pi}{3}R^3\left[(1-t^3) + \frac{3}{4}\left(\frac{L}{R}\right)(1-t^2) + \frac{3}{32}\left(\frac{L}{R}\right)^2(1-t)\right]. \tag{8}$$

## III. NUMERICAL DETERMINATION OF PERCOLATION THRESHOLD

### A. Background and procedure

Neda *et al.* [29] performed Monte Carlo simulations of isotropically oriented sticks in three dimensions and confirmed the prediction [28] that as $R/L \to 0$, the constant of proportionality in Eq. (1) is 1. Further, they derived a relationship between the critical number of high-aspect-ratio sticks and the stick aspect ratio based on their simulation results. The variable $s$ was introduced such that

$$s = q_p V_{ex} - 1. \tag{9}$$

Again, $q_p$ is the number of fibers per volume at percolation, i.e.,

$$q_p = \frac{N_c}{V}, \tag{10}$$

where $N_c$ is the number of sticks in the simulation cube at percolation, and $V$ is the volume of the simulation cube ($V=1$ in this case, so $q_p=N_c$). They showed that for $R/L < 0.06$, $\ln(s)$ varied linearly with $\ln(R/L)$, or

$$\ln(s) = a + b\ln\left(\frac{R}{L}\right). \tag{11}$$

Thus $s$ can be immediately written as

$$s = e^a\left(\frac{R}{L}\right)^b. \tag{12}$$

For simulations of sticks of length $L=0.15$ in a cube of side 1, they state that

$$s = \left(\frac{R}{L}\right)^{0.5764}. \quad (13)$$

It seems, from the plot of $\ln(s)$ vs $\ln(R/L)$ presented in Fig. 1 of their work, that the factor $e^a$ in Eq. (12) was omitted from the expression for $s$ given in the text.

The average number of bonds per site $B_c$ at percolation onsite is numerically equal to the total excluded volume [26], that is,

$$B_c = N_c V_{ex}. \quad (14)$$

Thus if the simulation cube is of unit volume, $B_c$ can be expressed as

$$B_c = 1 + s. \quad (15)$$

In this work we performed simulations to investigate the percolation threshold of systems of randomly distributed spherocylinders (sticks) of length $L=0.15$ and outer radius $R$ [see Fig. 1(b)] within a unit cube. Simulations were performed for values of $t$ equal to 0, 0.2, 0.3, 0.4, 0.5, and 0.6, respectively. The software package MATLAB [43] was used for all programming.

For the soft-core limit ($t=0$) the simulations were performed as follows using the same method employed by Neda *et al.* [29]. The coordinates of the center of each stick were generated uniformly between $-(L/2+R)$ and $1+(L/2+R)$. In order to obtain the correct isotropic distribution, each azimuthal angle $\gamma$ in the $x$-$y$ plane from the $x$ axis was generated randomly in the interval $(0,\pi)$ and the polar angle $\phi$ from the $z$ axis was chosen such that $\phi=\arccos(1-2\tau)$, where $\tau$ was a random number in the interval (0,1) [30]. The sticks were generated one at a time and each new stick was checked for intersection with those already inside the cube. Two sticks were considered to be intersecting if the shortest distance between them (i.e., the shortest distance between any two points along their lengths, the distance between their hemispheric end caps, or the shortest distance between an end cap of one stick and any point on the other) was less than or equal to $2R$. Percolation was defined as being reached when a cluster was found to span the cube in the $z$ direction. The number of cylinders inside the cube at percolation $N_c$ was recorded. When only a portion of a cylinder was found inside the cube at percolation, its contribution to $N_c$ was equal to the ratio of the cylinder volume inside the cube to its total volume.

For the hard-core simulations (values of $t>0$), each new stick was generated as described for the soft-core case, and checked for intersection with those already inside the cube. The cores of the sticks were not allowed to intersect, so if the shortest distance between any new stick and any stick already in the cube was less than or equal to $2r$, the stick was rejected and a new stick generated. Two sticks were considered to intersect if the shortest distance between them was less than or equal to $2R$ and greater than or equal to $2r$. Sticks were added one at a time in this manner until percolation was reached and the number of sticks within the cube at percolation, $N_c$ was recorded.

One hundred simulations were performed for each combination of $R$, $L$, and $t$ considered in the study and the mean and standard deviation values of $N_c$ were calculated from the results in each case. Since a unit cube was used in the simulations, $q_p=N_c$. The average values of $N_c$ were used to calculate $s$ values using Eq. (9). For $t=0$, $V_{ex}$ in Eq. (9) was calculated using Eq. (3) while Eq. (8) was used for the hard-core simulations (i.e., $t>0$).

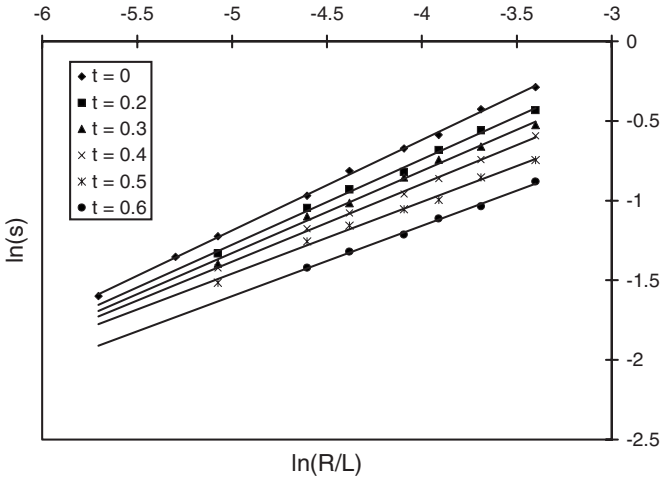


FIG. 2. $\ln(s)$ vs $\ln(R/L)$ for straight fibers ($L=0.15$).

### B. Results

Figure 2 shows the plot of $\ln(s)$ vs $\ln(R/L)$ for our systems ($L=0.15$). A linear relationship was observed between $\ln(s)$ and $\ln(R/L)$ for $L/R>30$ for all values of $t$ considered. From this result, the expression for $s$ can be written as

$$s = c_1\left(\frac{R}{L}\right)^{c_2}. \quad (16)$$

The number of fibers per unit volume at percolation is therefore given by the general expression

$$q_p = \frac{1 + c_1(R/L)^{c_2}}{V_{ex}}. \quad (17)$$

Table III below shows values of $c_1$ and $c_2$ derived from our simulations. By comparing our value of $c_2$ for $t=0$ with the result of Neda *et al.* [29], we see that our soft-core result is in excellent agreement with theirs.

Since $q_p$ can be expressed in the form of Eq. (17) it is clear that in the slender rod limit $R/L\to 0$, Eq. (5) is valid.

TABLE III. Values of $c_1$ and $c_2$ based on simulation results.

| $t$ | $c_1$ | $c_2$ |
|---|---|---|
| 0 | 5.231 | 0.569 |
| 0.2 | 4.080 | 0.537 |
| 0.3 | 3.506 | 0.517 |
| 0.4 | 2.876 | 0.488 |
| 0.5 | 2.213 | 0.451 |
| 0.6 | 1.844 | 0.443 |

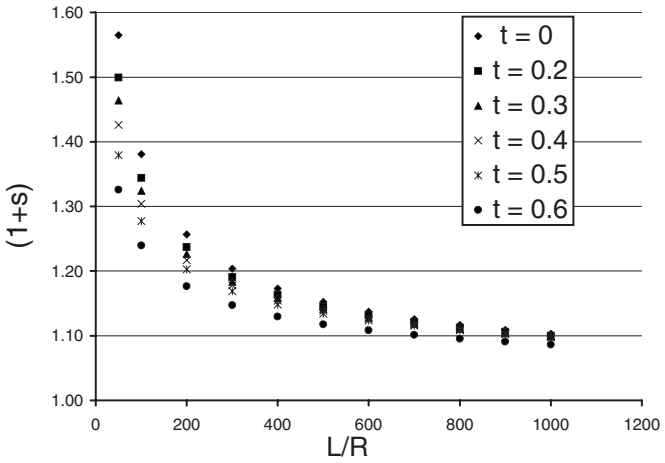


FIG. 3. $(1+s)$ vs $L/R$.

The rate of decay of the quantity $(1+s)$ is, however, very slow, and the results of the analytical solutions using Eq. (5) and Eq. (17) differ by 15% for aspect ratios as high as 500. It is therefore more appropriate to use the analytical solution of Eq. (17) than the popular approach, which assumes that the constant of proportionality is 1 for high-aspect-ratio fiber systems.

Figure 3 is a plot of $(1+s)$ vs aspect ratio for the values of $t$ considered in this study. The plot shows that our simulation results are also consistent with the results of Balberg and Binenbaum [39]. They conjectured that for cylinders of very large aspect ratio, the number of intersections per fiber $B_c$ [numerically equivalent to $(1+s)$ in our simulations], is dominated by aspect ratio rather than the parameter $t$, and in the limit $L/R \rightarrow 0$, $B_c$ is independent of $t$. Our results confirm that this is the case for the range of aspect ratios typically found in nanotube reinforced composites $(L/R > 400)$ since the values of $B_c$ over this range are within 4% of each other for the values of $t$ considered in our simulations. Thus based on this finding, for convenience we will use the values of $B_c$ for the soft shell $(t=0)$ case for all values of $t$ in the following section.

## IV. MODELING PERCOLATION IN NANOTUBE-REINFORCED COMPOSITES USING THE HARD-CORE APPROACH

The hard-core model is more suitable for modeling electrical percolation in systems where the conducting particles are not in physical contact and tunneling is the dominant charge transport mechanism. However, the more convenient soft-core model is often used, since it has been argued that for high-aspect-ratio fibers, the error introduced in doing so is small [41]. In this section we compare results of both modeling approaches to the problem of percolation in nanotubes reinforced composites.

A popular approach to calculating the nanotube volume fraction at percolation in nanotube reinforced composites is to use the analytical solution

$$\phi_c = \frac{V_{fiber}}{V_{ex}}, \tag{18}$$

where $V_{\text{fiber}}$ is the volume of the average nanotube or nanotubes bundle in the composite, and $V_{\text{ex}}$ is the excluded volume of a nanotube based on a soft-core approach. As previously discussed, a more accurate soft-core solution is

$$\phi_c = \frac{(1+s)V_{fiber}}{V_{ex}}, \tag{19}$$

where $s$ is calculated from Eq. (16) using the values of $c_1$ and $c_2$ for $t=0$ in Table III.

When using the hard-core approach to model percolation in systems of high-aspect-ratio fibers of length $L$ and radius $r$, the critical fiber volume fraction $\phi_c$ is the number of fibers per unit volume at percolation multiplied by the volume of the hard core, since the core represents the physical fiber. Thus

$$\phi_c = q_p V_{core}, \tag{20}$$

where the volume of the hard core, $V_{\text{core}}$, can be written as

$$V_{core} = \pi r^2 L + \frac{4}{3}\pi r^3. \tag{21}$$

Substituting for Eqs. (16) and (17) in Equation (18), the fiber volume fraction at percolation can be written as

$$\phi_c = \frac{(1+s)V_{core}}{V_{ex}}. \tag{22}$$

In the previous section we showed that for high aspect ratios, the quantity $(1+s)$ is constant for a given effective aspect ratio regardless of the value of $t$. The effective aspect ratio for the hard-core model is that of the fiber including the soft shell for the hard-core model (i.e., $L/R$) and the aspect ratio of the fiber itself (i.e., $L/r$) for the soft-core model. Since the typical aspect ratios in nanotube reinforced composites are reported to be in the range of several hundreds to several thousands [8,41] we can use the same value of $(1+s)$ for all values of $t$ for a given effective aspect ratio. In this section of the paper we computed $(1+s)$ from the soft shell $(t=0)$ results of the previous section.

We compare the experimentally derived electrical percolation threshold as reported by Ounaies *et al.* [8] with solutions obtained using both the soft-core and hard-core models. The approximate radius $r$ and length of the nanotubes were reported as 0.7 nm and 3 $\mu$m, respectively [8], which yields an aspect ratio of 4286. Experimental results were compared with analytical solutions calculated using Eq. (18), first assuming that the single nanotubes were uniformly dispersed within the matrix and then that the nanotubes were arranged in hexagonally close packed bundles of 7 and 19 nanotubes. For the analytical solution a bundle was approximated as an equivalent spherocylinder of length $L$ and radius $r$ equal to that of the bundle (see Fig. 4).

Table IV shows the results of the soft-core analytical solution using Eq. (18) as reported in the literature [8] along with the solution using Eq. (19) with the value of $s$ calculated based on the results of our own soft-core simulations, as reported in the previous section. Based on experiments, the percolation threshold was found to be 0.05%. Comparing this value to the analytical soft-core solution led to the conclusion that the single walled carbon nanotubes (SWNTs) within the polymer matrix were dispersed in very thin

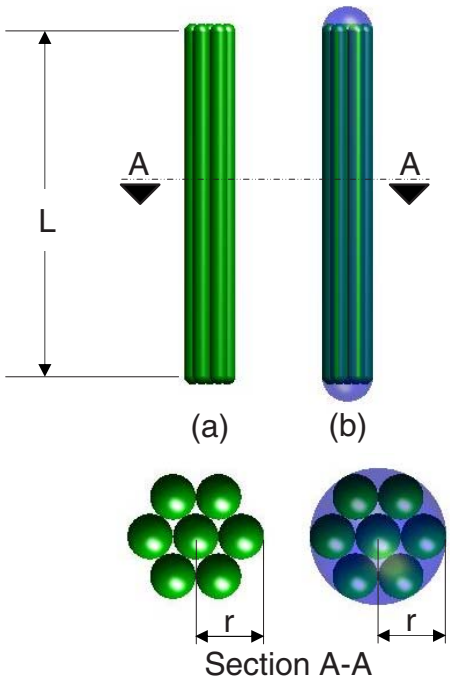


FIG. 4. (Color online) Schematic of (a) a bundle of seven nanotubes and (b) the equivalent spherocylinder used in calculation shown encasing the bundle

bundles made up of a few nanotubes since the experimental result was between the analytical solution for a single tube and a bundle of seven tubes [8].

For the hard-core analytical approach we consider the same three scenarios (a single tube and bundles of 7 and 19 tubes), and model the inner core in each case as a spherocylinder having the same dimensions as the single tube and equivalent bundles used in the soft-core model. Since the exact tunneling distance is not known, we consider various values of $t$ and compare the analytical results of Eq. (22) to the experimental percolation threshold. Figure 5 shows the analytical solution for percolation threshold for the three scenarios for a range of values of $t$. The values of $t$ which correspond to the experimental percolation threshold 0.05% were found in each case (see vertical dotted lines in Fig. 5) and used to calculate the soft-shell outer radius and thus the tunneling distance. These results are presented in Table V.

## V. DISCUSSION

It is clear that if the tunneling distance is indeed ~5 nm or less as suggested by Du *et al.* [33], the hard-core model

TABLE IV. soft-core analytical solution for percolation threshold for systems of uniformly distributed nanotubes and nanotubes bundles of length 3 $\mu$m.

| No. of nanotubes per bundle | Bundle radius $r$ (nm) | $L/r$ | Percolation threshold (vol %) Eq. (18) | Eq. (19) |
|---|---|---|---|---|
| 1 | 0.7 | 4286 | 0.023 | 0.024 |
| 7 | 2.1 | 1429 | 0.070 | 0.076 |
| 19 | 3.5 | 857 | 0.116 | 0.129 |

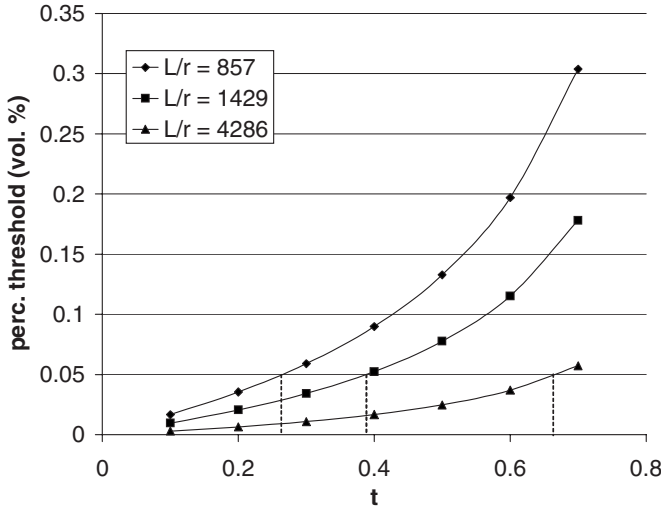


FIG. 5. Hard-core analytical solution for percolation threshold vs $t$ for nanotube bundles.

leads us to the same conclusion as the soft-core model, which is that the nanotubes within the composite in question are arranged in very thin bundles. In some instances the soft-core and hard-core models can yield similar results as illustrated in the previous section; however, the percolation threshold of the hard-core model is strongly dependent on the parameter $t$ and not only on the aspect ratio. Thus the error introduced in using a soft-core model for nanotube reinforced composites can be significant even for very high-aspect-ratio fibers. The soft-core model is more convenient to use since it depends only on the geometry and distribution of the fibers. The hard-core approach is the more accurate approach to modeling percolation in nanotube reinforced composites, although the model is more difficult to implement if the tunneling distance for the material is not known.

## VI. CONCLUSIONS AND FUTURE WORK

The relationship between percolation threshold and excluded volume for systems of both soft-core and hard-core fibers was investigated using Monte Carlo simulations. In all cases the percolation threshold was found to be inversely proportional to excluded volume, with the constant of proportionality being one in the limit $R/L \rightarrow 0$. For high-aspect-ratio fibers, the constant of proportionality was shown to be dominated by aspect ratio with little variation in the values obtained with respect to the parameter $t$ for a given aspect ratio.

TABLE V. soft-core analytical solution for percolation threshold for systems of uniformly distributed nanotubes and nanotubes bundles of length 3 $\mu$m.

| No. nanotubes per bundle | Bundle radius $r$ (nm) | $t$ | $R$ (nm) | Tunneling distance $2(R-r)$ (nm) |
|---|---|---|---|---|
| 1 | 0.7 | 0.67 | 1.04 | 0.69 |
| 7 | 2.1 | 0.39 | 5.38 | 6.57 |
| 19 | 3.5 | 0.265 | 13.21 | 19.42 |

A hard-core modeling approach is more appropriate for modeling composite materials in which the main charge transport mechanism is tunneling. In this paper we have applied this model to nanotube reinforced composites and have shown that the hard-core model yields results similar to those obtained using a soft-shell approach, but that the results are strongly dependent on the tunneling distance.

If the fiber geometry and distribution and the tunneling distance are known, the hard-core model can be applied to predict the electrical percolation threshold in a composite reinforced with high-aspect-ratio fibers. Since it is difficult to determine the tunneling distance experimentally, a useful application of the hard-core modeling technique would be to determine the likely tunneling distance given the fiber geometry, distribution, and the experimentally derived percolation threshold. This can be achieved by finding the value of the parameter $t$ which results in a match between the value of experimental percolation threshold obtained and the analytical solution. Future work will include the use of this approach to investigate the effect of parameters such as fiber type, functionalization method, and molecular weight of the polymer matrix on the tunneling distance in polymer nanocomposites.

Paper II of this work investigates the effect of the inherent waviness of embedded nanotubes on the onset of percolation in nanotubes reinforced composites.

## ACKNOWLEDGMENTS

This work was supported in part by a grant of computing time from the Ohio Supercomputer Center (L.B.), and from the U.S. Department of Energy BATT Program under Contract No. DE-AC02-05CH1123 (A.M.S.).

[1] R. Andrews *et al.*, Macromol. Mater. Eng. **287**, 395 (2002).
[2] J. M. Benoit *et al.*, Synth. Met. **121**, 1215 (2001).
[3] M. J. Biercuk *et al.*, Appl. Phys. Lett. **80**, 2767 (2002).
[4] G. B. Blanchet, C. R. Fincher, and F. Gao, Appl. Phys. Lett. **82**, 1290 (2003).
[5] J. N. Coleman *et al.*, Phys. Rev. B **58**, R7492 (1998).
[6] B. E. Kilbride *et al.*, J. Appl. Phys. **92**, 4024 (2002).
[7] E. Kymakis, I. Alexandou, and G. A. J. Amaratunga, Synth. Met. **127**, 59 (2002).
[8] Z. Ounaies *et al.*, Compos. Sci. Technol. **63**, 1637 (2003).
[9] P. Potschke, T. D. Fornes, and D. R. Paul, Polymer **43**, 3247 (2002).
[10] J. Sandler *et al.*, Polymer **40**, 5967 (1999).
[11] K. Yoshino *et al.*, Fullerene Sci. Technol. **7**, 695 (1999).
[12] S. Rul *et al.*, Acta Mater. **52**, 1061 (2004).
[13] V. Favier *et al.*, Polym. Eng. Sci. **37**, 1732 (1997).
[14] V. Favier *et al.*, Acta Mater. **45**, 1557 (1997).
[15] X. Cheng and A. M. Sastry, Mech. Mater. **31**, 765 (1999).
[16] X. Cheng, A. M. Sastry, and B. E. Layton, J. Eng. Mater. Technol. **123**, 12 (2001).
[17] X. Cheng *et al.*, J. Eng. Mater. Technol. **121**, 514 (1999).
[18] A. M. Sastry, X. Cheng, and C. W. Wang, J. Thermoplast. Compos. Mater. **11**, 288 (1998).
[19] A. M. Sastry, S. B. Choi, and X. Cheng, J. Eng. Mater. Technol. **120**, 280 (1998).
[20] C. Wang *et al.*, J. Eng. Mater. Technol. **121**, 503 (1999).
[21] C. W. Wang, L. Berhan, and A. M. Sastry, J. Eng. Mater. Technol. **122**, 450 (2000).
[22] C. W. Wang and A. M. Sastry, J. Eng. Mater. Technol. **122**, 460 (2000).
[23] L. Berhan and A. M. Sastry, J. Compos. Mater. **37**, 715 (2003).
[24] L. Berhan, Y. B. Yi, and A. M. Sastry, J. Appl. Phys. **95**, 5027 (2004).
[25] L. Berhan *et al.*, J. Appl. Phys. **95**, 4335 (2004).
[26] I. Balberg *et al.*, Phys. Rev. B **30**, 3933 (1984).
[27] I. Balberg, N. Binenbaum, and N. Wagner, Phys. Rev. Lett. **52**, 1465 (1984).
[28] A. L. R. Bug, S. A. Safran, and I. Webman, Phys. Rev. Lett. **54**, 1412 (1985).
[29] Z. Neda, R. Florian, and Y. Brechet, Phys. Rev. E **59**, 3717 (1999).
[30] Y. B. Yi and A. M. Sastry, Proc. R. Soc. London, Ser. A **460**, 2353 (2004).
[31] Y. B. Yi, C. W. Wang, and A. M. Sastry, J. Electrochem. Soc. **151**, A1292 (2004).
[32] J. M. Benoit, B. Corraze, and O. Chauvet, Phys. Rev. B **65**, 241405 (2002).
[33] F. M. Du *et al.*, Macromolecules **37**, 9048 (2004).
[34] I. Balberg, Carbon **40**, 139 (2002).
[35] I. Balberg *et al.*, Int. J. Mod. Phys. B **18**, 2091 (2004).
[36] D. Toker *et al.*, Phys. Rev. B **68**, 041403 (2003).
[37] A. L. R. Bug *et al.*, Phys. Rev. Lett. **55**, 1896 (1985).
[38] G. S. Grest *et al.*, Phys. Rev. A **33**, 2842 (1986).
[39] I. Balberg and N. Binenbaum, Phys. Rev. A **35**, 5174 (1987).
[40] A. A. Ogale and S. F. Wang, Comput. Struct. **46**, 379 (1993).
[41] M. Foygel *et al.*, Phys. Rev. B **71**, 104201 (2005).
[42] M. Grujicic, G. Cao, and W. N. Roy, J. Mater. Sci. **39**, 4441 (2004).
[43] The MathWorks, *Matlab Programming Version 7*, 2004.